15th Australasian Fluid Mechanics Conference
The University of Sydney, Sydney, Australia
13-17 December 2004

Linear stability of natural convection on an evenly heated vertical wall

G. D. McBain and S. W. Armfield

School of Aerospace, Mechanical, & Mechatronic Engineering
The University of Sydney, Darlington NSW 2006 AUSTRALIA

Abstract

A collocation technique is applied to the equations governing the linear stability of the anabatic layer on an evenly heated vertical wall in a stratified fluid. Marginal stability curves and critical heat fluxes are obtained for Prandtl numbers from 0 to 1000. As in other cases of vertical natural convection, two kinds of instability are observed, depending on the Prandtl number: at lower Prandtl numbers, the modes are short slow waves and the critical parameter is roughly proportional to the local Reynolds number, whereas at higher Prandtl numbers, the critical Reynolds number decreases rapidly and the waves are longer and faster.

Introduction

One of the simplest solutions of the Oberbeck [14] equations of natural convection was discovered by Prandtl [15, pp. 422–425]. It describes the flow parallel to a vertical (or inclined) plane held at a constant temperature difference above the neighbouring stratified fluid. The linear stability of this flow has been studied by Gill & Davey [7].

A more realistic boundary condition, however, is that of a uniform heat flux at the wall. Since Prandtl's [15] base solution is independent of height, it also applies in this case. The flow may be realized in a cavity with evenly heated and cooled vertical walls [9], and its mass transfer-analogue occurs in electrochemical cells [6]. The stability properties differ, however, due to the replacement of the Dirichlet condition, $\theta(0) = 0$, on the thermal perturbation with a Neumann one, $\theta'(0) = 0$. The authors have recently investigated the linear stability of this modified problem for Prandtl number $\sigma = 7$ [11], and shown that both the critical Reynolds number and the form of the critical disturbance agree with direct numerical simulations. The present paper extends the linear stability results to the range $0 \leqslant \sigma \leqslant 10^3$.

Mathematical formulation

Let the x-axis be normal to the wall and the y-axis vertical. Denote the fluid properties by ν, α, and β for the coefficients of kinematic viscosity, thermometric conductivity, and thermal expansion, respectively. Denote the normal temperature gradient at the wall by Γ_w, the far-field stratification by Γ_s, and the gravitational field strength by g. Then if

$$\delta = \left(\frac{4\alpha\nu}{g\beta\Gamma_s}\right)^{1/4} \tag{1}$$

$$U = \Gamma_w \left(\frac{4g\beta}{\nu}\right)^{1/4} \left(\frac{\alpha}{\Gamma_s}\right)^{3/4} = \frac{2\alpha\Gamma_w}{\Gamma_s\delta} \tag{2}$$

$$\Delta T = \Gamma_w\delta \tag{3}$$

are the scales for length, speed, and temperature [7, 11], the governing parameters are the Prandtl number, $\sigma = \nu/\alpha$ and the Reynolds number

$$R = \frac{U\delta}{\nu} = \frac{2\Gamma_w}{\Gamma_s\sigma}, \tag{4}$$

and the Oberbeck equations governing the evolution of the velocity $\mathbf{u}$, pressure p, and temperature T in time t are

$$R\left(\frac{\partial}{\partial t} + \mathbf{u}\cdot\nabla\right)\mathbf{u} = -R\nabla p + \nabla^2\mathbf{u} + 2T\hat{\mathbf{e}}_y \tag{5}$$

$$R\sigma\left(\frac{\partial}{\partial t} + \mathbf{u}\cdot\nabla\right)T = \nabla^2 T, \tag{6}$$

subject to the velocity vanishing at the wall

$$\mathbf{u} = \mathbf{0} \qquad (x = 0), \tag{7}$$

the wall heat flux being specified

$$\frac{\partial T}{\partial x} = -1 \qquad (x = 0), \tag{8}$$

and general decay far from the wall

$$|\mathbf{u}|, \left(T - \frac{2y}{R\sigma}\right) \sim 0 \qquad (x \to \infty). \tag{9}$$

The system (5)–(9) admits Prandtl's [15, 7, 11] steady one-dimensional solution $\mathbf{u} = V(x)\hat{\mathbf{e}}_y$, $T = \Theta(x) + 2y/R\sigma$ where

$$V(x) = \mathrm{e}^{-x}\sin x \tag{10}$$

$$\Theta(x) = \mathrm{e}^{-x}\cos x. \tag{11}$$

The stability of small plane perturbations with streamwise wavenumber κ and wave speed c of the form

$$\delta\mathbf{u} = \Re\hat{\mathbf{e}}_z \times \nabla\psi(x)\mathrm{e}^{\mathrm{i}\kappa(y-ct)} \tag{12}$$

$$\delta T = \Re\theta(x)\mathrm{e}^{\mathrm{i}\kappa(y-ct)} \tag{13}$$

are governed by [7]

$$[E^2 + \mathrm{i}\kappa R\{(V-c)E + V''\}]\psi + 2\mathrm{D}\theta = 0 \tag{14}$$

$$\left[2\mathrm{D} - \mathrm{i}\kappa R\sigma\Theta'\right]\psi + [E + \mathrm{i}\kappa R\sigma(V-c)]\theta = 0, \tag{15}$$

subject to

$$\psi(0) = \psi'(0) = \theta'(0) = \psi(\infty) = \theta(\infty) = 0, \tag{16}$$

where $\mathrm{D} = \mathrm{d}/\mathrm{d}x$ and $\mathrm{E} = \kappa^2 - \mathrm{D}^2$. For the temporal linear stability problem, κ is taken as real, ψ and θ are the eigenvectors, and c is the complex eigenvalue.

Discretization and solution procedure

As in the previous study [11], (14)–(15) were discretized using orthogonal collocation based on weighted generalized Laguerre functions, the algebraic generalized eigenvalue problem $(L - cM)q = 0$ converted to standard form as $(M^{-1}L - c)q = 0$, and solved by the QR algorithm. The flow is regarded as unstable at a given σ, R, and κ if any part of the c-spectrum lies in the upper-half complex plane.

This approach needed modification at $\sigma = 0$, however, since then c disappears from (15); i.e. the 'mass matrix' M becomes singular, prohibiting the usual conversion to standard form. Instead, we used a shift-and-invert technique [1, 12] with the shift taken near the critical complex wave speed found for small but finite Prandtl numbers. The zero Prandtl number limit for this problem differs from that for the isothermal slot [3], since there the ψ-perturbation equation (14) becomes uncoupled from the θ-equation (15); the reason is that the length scale there is fixed by the slot width, but here (1) depends on α.

A Reynolds number close to both a value of R for which the flow is stable and one for which it is unstable is a *marginal* Reynolds number for that σ and κ; the locus of marginal Reynolds numbers and κ is the *stability margin*. Margins for various σ were traced using our adaptive skirting algorithm [10].

The least marginal Reynolds number for a given κ and σ is the critical Reynolds number for that σ number. After roughly locating the turning points of the margins, the critical Reynolds numbers were found by Golden Section search [8, p. 37].

The method convergences exponentially (as is to be expected from an orthogonal collocation method) for number of collocation points n up to about 60; for higher n, a levelling-off occurs, probably due to the high condition number of the differentiation matrices. This is illustrated in figure 1, which shows the

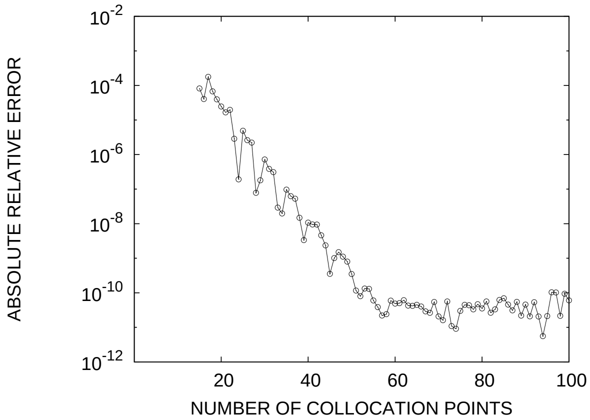

Figure 1: Convergence of the collocation method with bisection for the marginal Reynolds number at $\sigma = 7$ and $\kappa = 0.4612$.

absolute relative error in the marginal Reynolds number computed for $\sigma = 7$ and $\kappa = 0.4612$ (taking the true value to be $R = 8.581336650$ as assessed from all data at $10 < n < 100$).

Another check on the method and code was made by reproducing Gill & Davey's results [7] for the critical Reynolds numbers with the fixed temperature boundary condition; i.e. they assumed $T(0) = 1$ in place of (8), and so replaced $\theta'(0) = 0$ in (16) with $\theta(0) = 0$. Their results, originally obtained with a finite difference shooting method, were found to be correct to the stated accuracy of three significant figures.

All computations were programmed in Octave [5] and executed on a heterogeneous openMosix cluster. Computations at each Prandtl number were performed serially, but several such programs were executed simultaneously.

Results

The variation of critical Reynolds number with Prandtl number is plotted in figure 2 and some critical modes in figure 3.

At $\sigma = 0$ the marginal stability curve is simple (figure 4 *a*) but by $\sigma = 0.1$ a second lobe, representing a second mode of instability, appears at small wavenumbers (figure 4 *b*). The crit-

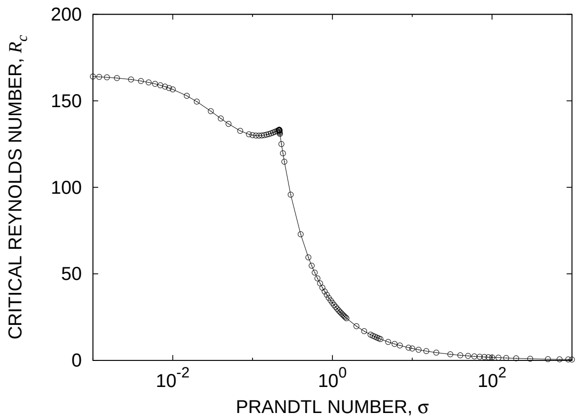

Figure 2: Critical Reynolds numbers.

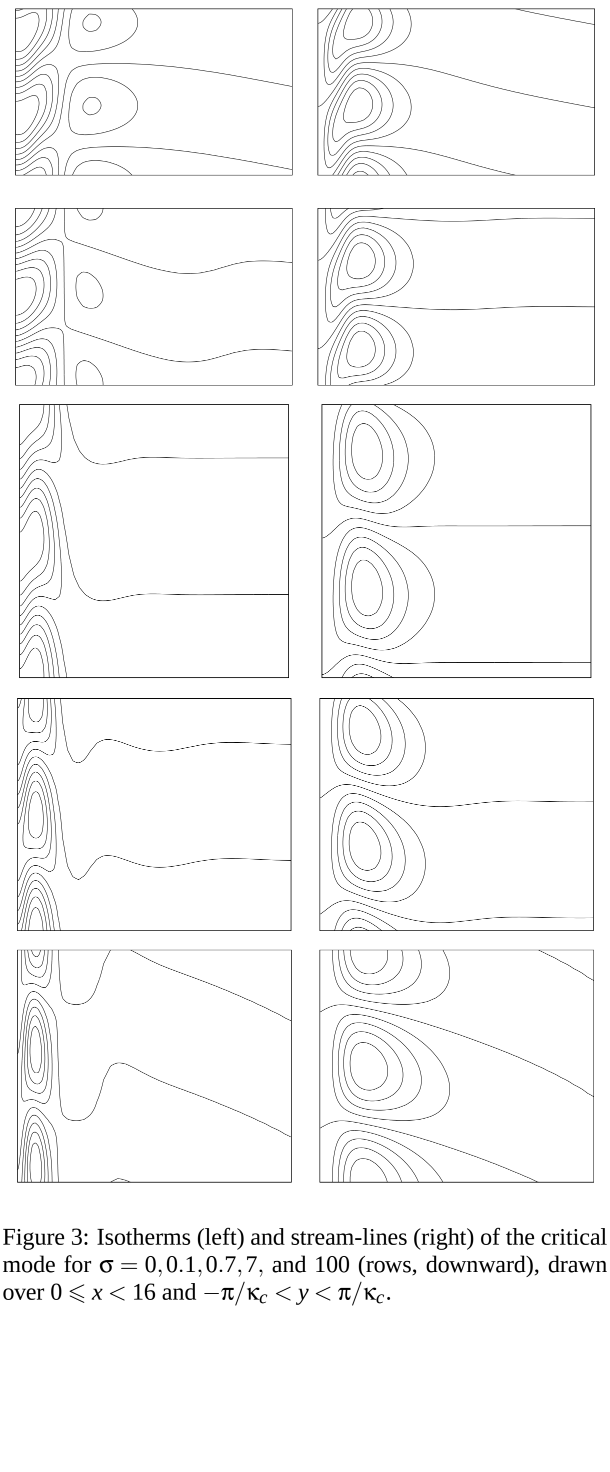

Figure 3: Isotherms (left) and stream-lines (right) of the critical mode for $\sigma = 0, 0.1, 0.7, 7$, and 100 (rows, downward), drawn over $0 \leqslant x < 16$ and $-\pi/\kappa_c < y < \pi/\kappa_c$.

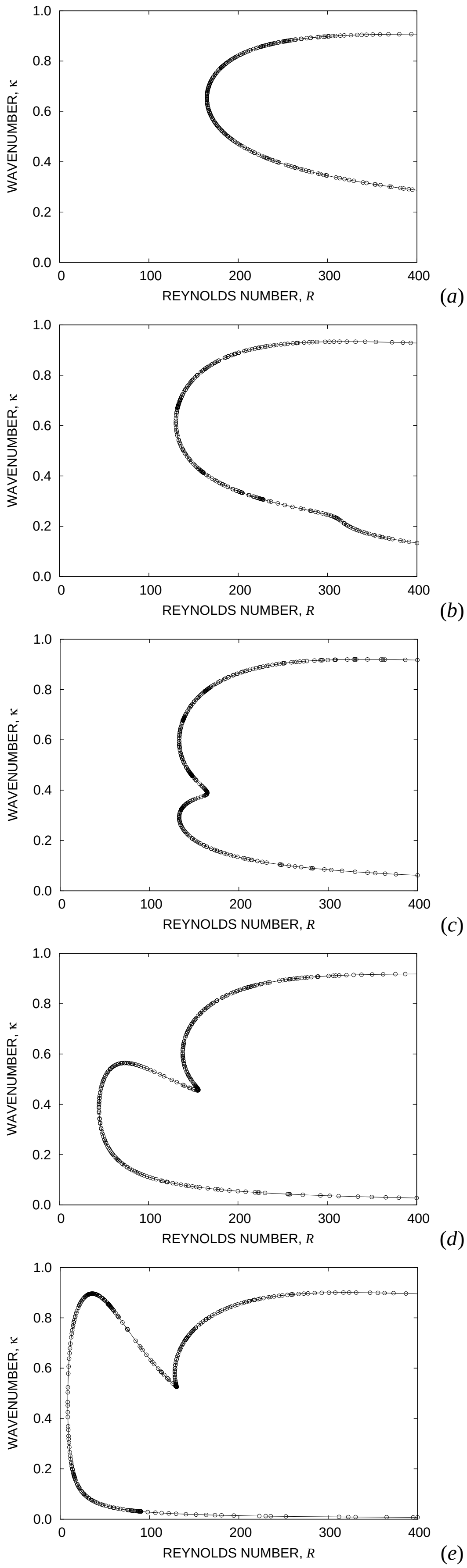

Figure 4: Marginal stability curves: $\sigma = (a)$ 0, (b) 0.1, (c) 0.2163, (d) 0.7, (e) 7.

ical Reynolds number decreases with increasing σ, reaching a minimum of about 130 near $\sigma = 0.12$, then increases again (figure 2). The critical Reynolds number of the second mode decreases faster with increasing Prandtl number, and there is a cusp in the critical curve at $R_c = 133$ near $\sigma = 0.2163$ at which the second mode passes the first (figures 2, 4 c). Thereafter, R_c enters a steep decline which continues up to the highest Prandtl numbers investigated ($\sigma = 10^3$).

Discussion

The phenomenon of the low Prandtl number mode of instability giving way to one with longer wavelength and greater speed (see figure 5) also occurs in the linear stability of convection in

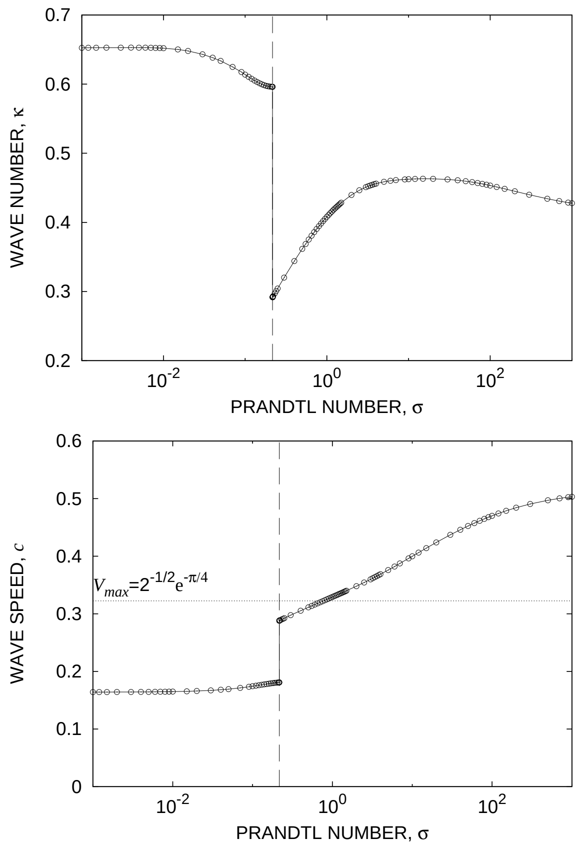

Figure 5: Critical wave numbers (above) and wave speeds (below, also showing the maximum speed of the base flow). The dashed vertical line marks $\kappa = 0.2163$.

a vertical slot [4, 12], in a stratified vertical slot [2], in the fixed-temperature-excess plate problem [7], and for a hot isothermal plate in a cold isothermal fluid [13]. Here, however, the transition occurs at quite a low Prandtl number: $\sigma \approx 0.216$; cf. $\sigma = 12.454$ for the slot [12] and somewhere in $0.4 < \sigma < 0.72$ for the fixed-temperature-excess plate [7]. Roughly speaking, we suspect this is because the Neumann condition on the temperature perturbation is less restricting to the 'thermal' mode. We call the first and second modes 'hydrodynamic' and 'thermal' since the first sets in at roughly a constant boundary layer Reynolds number, while the latter is strongly dependent on the Prandtl number.

In order to investigate the effect of the thermal boundary condition on the stability of the anabatic layer, our critical Reynolds numbers are compared with those of Gill & Davey [7] in figure 6. It is evident that the low Prandtl number ($\sigma < 0.2163$) critical mode is slightly stabilized by the change to the

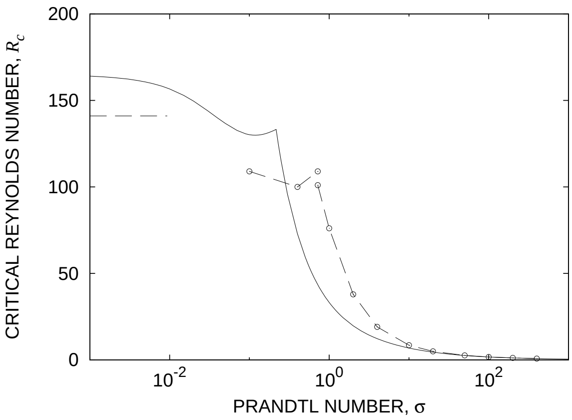

Figure 6: Comparison of critical Reynolds numbers for the linear stability of a vertical anabatic layer for heat flux (present work, curve) and temperature (Gill & Davey [7], points joined by line segments) thermal boundary conditions.

flux boundary condition, though at moderate Prandtl numbers ($0.2163 < \sigma <\sim 10^1$–$10^2$) the base flow is destabilized with respect to the 'thermal' mode by the change: the critical Reynolds numbers at large Prandtl numbers are less, and this mode becomes the critical one at a lower Prandtl number. At large Prandtl numbers, the difference disappears; e.g. Gill & Davey's $R_c = 1.70$ at $\sigma = 100$, which coincides with the figure in table 1. This is because the hot and cold spots in the critical modes are increasingly localized, away from the wall and near the maximum of the base velocity profile; both the value and gradient of the temperature perturbation are small near the wall so the two boundary conditions are equivalent. This may be seen by comparing Gill & Davey's figure 11 with the lower isotherm plots in our figure 3.

Conclusions

The specially developed collocation method based on generalized Laguerre functions provides accurate solutions to the linear stability equations for this flow with modest computational requirements.

Like other vertical natural convection flows, the anabatic layer on an evenly heated wall in a stratified fluid has two different critical modes, depending on the Prandtl number.

The present flow system is particularly suitable for linear stability studies, since, unlike the boundary layer in an isothermal fluid, it has a parallel base flow; unlike the unstratified slot, it has boundary layer behaviour in the base solution; and compared to the stratified slot, it depends on only two parameters rather than three.

For future reference, some selected critical values are listed in table 1.

σ	R	κ	c
0	164.89414	0.6523	0.1641
10^{-3}	164.0357	0.6525	0.1642
10^{-2}	156.6220	0.6520	0.1650
10^{-1}	130.19156	0.6138	0.1743
(0.2163)	(133.2506)	(0.5962)	(0.1809)
0.2163	133.2403	0.2917	0.2882
0.7	44.48526	0.3858	0.3200
7	8.58134	0.4612	0.3874
10	6.859748	0.4625	0.3999
10^2	1.7001183	0.4533	0.4702
10^3	0.4841815	0.4278	0.5033

Table 1: Critical data. The data are believed accurate to the stated precision.

Acknowledgements

McBain and Armfield acknowledge funding from The University of Sydney's Sesqui Postdoctoral Fellowship scheme and the Australian Research Council's Discovery scheme, respectively.

References

[1] Bai, Z., Demmel, J., Dongarra, J., Ruhe, A. and van der Vorst, H., editors, *Templates for the Solution of Algebraic Eigenvalue Problems*, SIAM, Philadelphia, 2000.

[2] Bergholz, R. F., Instabilities of steady natural convection in a vertical fluid layer, *J. Fluid Mech.*, **84**, 1978, 743–768.

[3] Birikh, R. V., On small perturbations of a plane parallel flow with cubic velocity profile, *J. appl. Math. Mech.*, **30**, 1966, 432–438.

[4] Birikh, R. V., Gershuni, G. Z., Zhukhovitskii, E. M. and Rudakov, R. N., On oscillatory instability of plane–parallel convective motion in a vertical channel, *J. appl. Math. Mech.*, **36**, 1972, 707–710.

[5] Eaton, J. W., *GNU Octave Manual*, Network Theory, 2002.

[6] Eklund, A., Alavyoon, F., Simonsson, D., Karlsson, R. I. and Bark, F. H., Theoretical and experimental studies of free convection and stratification of electrolyte in a copper refining cell, *Electrochimica Acta*, **36**, 1991, 1345–1354.

[7] Gill, A. E. and Davey, A., Instabilities of a buoyancy driven system, *J. Fluid Mech.*, **35**, 1969, 775–798.

[8] Greig, D. M., *Optimisation*, Longman, 1980.

[9] Kimura, S. and Bejan, A., The boundary layer natural convection regime in a rectangular cavity with uniform heat flux from the side, *J. Heat Transfer*, **106**, 1984, 98–103.

[10] McBain, G. D., Skirting subsets of the plane, with application to marginal stability curves, *ANZIAM J.*, **45(E)**, 2004, C78–C91.

[11] McBain, G. D. and Armfield, S. W., Instability of the buoyancy boundary layer on an evenly heated vertical wall, submitted for publication in J. Fluid Mech., 2004.

[12] McBain, G. D. and Armfield, S. W., Natural convection in a vertical slot: Accurate solution of the linear stability equations, *ANZIAM J.*, **45(E)**, 2004, C92–C105.

[13] Nachtsheim, P. R., Stability of free-convection boundary-layer flows, Tech. Note D-2089, NASA, 1963.

[14] Oberbeck, A., Ueber die Wärmeleitung der Flüssigkeiten bei Berücksichtigung der Strömungen infolge von Temperaturdifferenzen, *Ann. Phys. Chem.*, **7**, 1879, 271–292, neue Folge.

[15] Prandtl, L., *Essentials of Fluid Dynamics*, Blackie, 1952.